

# Hydroxyapatite coating by sol–gel on Ti–6Al–4V alloy as drug carrier

Eduardo Peón Avés · Gaston Fuentes Estévez ·  
Marcia Soares Sader · Juan C. Galván Sierra ·  
Julio C. Llopiz Yurell · Ivan N. Bastos ·  
Gloria D. Almeida Soares

Received: 20 June 2008 / Accepted: 2 October 2008 / Published online: 18 December 2008  
© Springer Science+Business Media, LLC 2008

**Abstract** In this study Ti–6Al–4V samples were used as substrates and Ca–P layers were deposited using sol–gel technique and covered by spin-coating. The efficiency of hydroxyapatite (HA) coatings as drug carrier was also evaluated by immersion in gentamicin sulphate solution and the release profiles were obtained by cumulative method of the coating samples. Three non-linear mathematical methods were employed in order to discuss a possible mechanism to lead the drug release. Physical chemical techniques showed the presence of the typical absorption bands of calcium phosphates by infrared spectroscopy while X-ray diffraction peaks matched up with hydroxyapatite patterns. Microstructural techniques (SEM, EDS) help to confirm the hydroxyapatite coating by surface aspect and Ca/P ratio (1.64). The best fitting according statistical results explained each stage of the released profiles and correspond to a mixture of short initial burst

effect plus drug dissolution with a specific kinetic and the diffusion of the gentamicin solid particles.

## 1 Introduction

The implementation of a sol–gel methodology enables a number of advantages over other coating techniques such as: increased homogeneity as mixing occurs on the atomic level; reduced sintering temperatures due to small particle size; ability coat complex shapes easily; and numerous deposition techniques that can be employed to produce coatings as dip, spin or spray coating [1]. This produces coatings comparable in thickness with sputter deposition which are typically less than 1  $\mu\text{m}$ . The development of hydroxyapatite (HA) using the sol–gel route is based on the work of Liu et al. [2, 3] on powder production, which was applied with further modification for coating production using the spin-coating technique.

A variety of prophylactic and therapeutic techniques have been designed to reduce the incidence and impact of infection. Conventional treatment using systemic antibiotics is expensive, prone to complications and often unsuccessful. Gentamicin is one of the most common antibiotics for incorporation in the biomedical devices due to its wide antibacterial spectrum and because, unlike many antibiotics, it is stable at the high temperatures. In vitro release assays require a large amount of measures of gentamicin concentration in different test solutions, so quick, reliable and inexpensive methods for its quantification are needed [4]. A wide variety of methods can be used to quantify aminoglycoside antibiotics, including enzymatic immunoassay and also chromatographic and spectrophotometric methods. Chromatographic methods are the ones used in most

---

E. P. Avés · G. F. Estévez (✉)  
Department of Ceramic and Composites, Centro de  
Biomateriales, Universidad de La Habana, Havana, Cuba  
e-mail: gastonfe@biomat.uh.cu

M. S. Sader · G. D. A. Soares  
Escola Politécnica Engenharia Metalúrgica e de Materiais,  
COPPE/UFRJ, Rio de Janeiro, Brazil

J. C. G. Sierra  
CENIM, CSIC, Madrid, Spain

J. C. L. Yurell  
Institute of Materials Science and Technology, Universidad de  
La Habana, Havana, Cuba

I. N. Bastos  
Polytechnic Institute, Universidade do Estado do Rio de Janeiro,  
NovaFriburgo, Rio de Janeiro, Brazil

pharmacopoeias for the quantitative analysis of gentamicin. In spite of its reliability the main drawback of chromatographic methods is that it is time-consuming. Radio-enzymatic and radioimmunoassays methods, also quite reliable, are very expensive. Spectrophotometric methods are usually rapid, sensitive and more economical [5].

In the present communication preliminary results of a gentamicin release from Ti–Al–V alloy with HA coatings are shown integrated in the one that aspects are contemplated as diverse as they are the preparation, the design and the characterization of HA coatings on Ti alloys, for possible biomedical applications and their evaluation as drug carrier.

## 2 Materials and methods

In this study, 1 cm<sup>2</sup> Ti–6Al–4V samples, 1 mm of thickness, were used as substrates. Alloys samples were submitted to mechanical blasting process with # 60 mesh alumina powder (Alumina Azul no. 1, QM). The samples were etched with an acid solution containing hydrogen peroxide and hydrofluoric acid [6] to remove Al<sub>2</sub>O<sub>3</sub> particles and to produce a homogeneous rough surface and ultrasonically cleaned in acetone for 15 min, alcohol for 10 min, and water for 5 min. The sol–gel procedure has been detailed by Liu et al. [2, 3]. Briefly, triethyl phosphite (Aldrich) was first hydrolyzed for 24 h with a fixed amount of distilled water under vigorous stirring. A stoichiometric amount of calcium nitrate (Aldrich), 4 mol/l solution, was added into the hydrolyzed phosphite solution. Then, the resulting mixture was agitated for additional 30 min and aged for 24 h. The coating on the metallic substrate with the sol–gel solution was prepared by spin-coating, with a speed of 4200 rpm for 9 s and dried at 80°C. The method of thermal treatment, consistent in a variant of the control rate thermal treatment (CRTT) [7] with the object that crystallization and densification of the coating HA be also controlled their texture characteristics, it was applied at 450°C for 5 h in vacuum.

The coatings layers obtained were characterized by infrared spectroscopy (FTIR-ABB Bomem Inc., MB series) equipped with reflectance stage, recorded in the range of 400–4000 cm<sup>-1</sup>, and X-ray diffraction (XRD-RIGAKU—Miniflex), performed with CuK $\alpha$  radiation (30 kV, 50 mA). Data was acquired from 20° to 60° (2 $\theta$ ). The morphologic characteristics and elementary composition of the HA coating obtained was investigated by scanning electron microscopy (SEM-JEOL JSM-6460LV) with energy dispersive spectroscopy associated (EDS-Noran System Six 200). The efficiency of HA coatings as drug carrier was also evaluated by immersion in gentamicine sulfate solution with and without stirring.

Gentamicin sulfate (Garamicina<sup>®</sup>, 140 mg/ml solution) was manufactured by Scheuring and Plough (Brazil). All gentamicin concentrations were determined by UV spectrophotometric method (Cary 1E, Variant, USA). Five independent experiments were carried out for the studies. Diffusion of the antibiotic from HA coating metallic substrates was studied in vitro. The coating alloys samples were immersed in 20 ml of 200 and 500 ppm solutions, with (S2/200 ppm and S5/500 ppm) and without (N2/200 ppm and N5/500 ppm) stirring. Then, the HA coating metallic substrates doped with gentamicine sulfate were immersed in 10 ml of deionized water and maintained thermostatically at 37°C. All the solutions were removed every half and hour and replaced by fresh medium. The mathematical models evaluated in this work were Weibull distribution (Eq. 1) [8–10], the logistic function (Eq. 2) [10] and TF model (Eq. 3) [5]

$$M_t = M_\infty [1 - \exp(-\alpha t^\beta)] \quad (1)$$

$$M_t = \alpha / [1 + \exp(\beta t / \gamma)] \quad (2)$$

$$M_t = M_b + M_\infty (1 - e^{-mt}) + kt^{1/2} \quad (3)$$

with  $M_t$  the percentage drug dissolved at time  $t$ ,  $M_\infty$  the percentage drug dissolved at infinite time and usually set equal to 100% in all cases. For Eq. 1  $\alpha$  means the scale factor and  $\beta$  the shape factor. In case of Eq. 2,  $\alpha$  is the value of the horizontal asymptote as  $t$  approaches infinity ( $t \rightarrow \infty$ );  $\beta$  the time at which  $M_t = \alpha/2$  and  $\gamma$  the scale parameter on the time axis which represents the distance on the time axis between  $\beta$  and the point where the response is  $\alpha/(1 + e^{-1}) \approx 0.73\alpha$ . But in Eq. 3 the interpretation of terms is as follows: the first term on the right-hand side,  $M_b$ , is associated with the initial burst effect, the second term  $M_\infty(1 - e^{-mt})$ , is associated with the kinetics of a dissolution process and the third term could be associated with a Fickian diffusion of a drug solid particle in its diluted solution.

Experimental data were analyzed by a non-linear least-squares regression, using the Statgraphics Plus 5.1 (Professional edition, Statistical Graphics Corp, USA) and Origin 7.0 (Origin Lab Corp, Northampton, MA, USA). The model that best explains the experimental data is the one that shows the minimal value for the SSR. However, since a larger number of model parameters could lead to a higher probability of obtaining a smaller SSR value, it was necessary to use a discriminatory criterion that was independent of the number of parameters that each model had. For this reason, the Akaike Information Criterion (AIC) was applied and it can be defined as  $AIC = N (\ln SSR) + 2p$  where  $N$  is number of experimental data points, SSR is the sum of the squared residuals and  $p$  is the number of parameters. The model that shows the smallest value for the AIC is the one which, statistically, describes the best the drug release mechanism [11].

### 3 Results and discussion

The slightly porous HA coating were initially analyzed by FTIR (Fig. 1). The characteristic bands of the  $\nu_2(\text{PO}_4^{3-})$  is observed at 566 and 601  $\text{cm}^{-1}$ ,  $\nu_1(\text{PO}_4^{3-})$  at 954  $\text{cm}^{-1}$ , and the  $\nu_3(\text{PO}_4^{3-})$  to the 1087 and 1022  $\text{cm}^{-1}$ . These bands indicate the classification of the polyhedrons of  $\text{PO}_4^{3-}$  in the structure of the glass. Besides, at 3566  $\text{cm}^{-1}$  a main vibration  $\nu(\text{OH}^-)$  is observed. The band at 628  $\text{cm}^{-1}$  is attributed to the  $\text{OH}^-$  groups [12]. In the coat obtained by sol-gel process the  $\text{CO}_3^{2-}$  incorporation was detected by the presence of the bands at 870  $\text{cm}^{-1}$ ,  $\delta(\text{CO}_3^{2-})$  reinforced with the contribution of P-OH bonds from HA, and the main stretching  $\text{CO}_3^{2-}$  at 1,422 and 1,460  $\text{cm}^{-1}$ , originally a double band, overposed by coupling vibrations due to crystal structure [13]. The XRD patterns shown in Fig. 2. The wide peak that appears in 26.40° (002), 32.35° (211), 32.50° (112), 32.60° (300) and 49.05° (213) were assigned to HA, according to the JCPDS 9-432 card. The

$\text{CaCO}_3$  phase in the coating might be due to the combination of calcium in the precursor with evolved  $\text{CO}_2$  arising from pyrolysis of organics in precursor during heating [12].

Figure 3 shows the HA coating morphology. The coating is porous and no cracks are found. The pores developed in the coating are believed to be a result of gas evolution during thermal decomposition. These pores seem to be connected to form a continuous network and the pore size ranging from 5 to 10  $\mu\text{m}$ . This morphology may be an advantage to permit the circulation of drug and physiological fluid. EDS analysis of HA coating on Ti alloys substrates can be observed in Fig. 4. It does not observe any peak of Ti, which help it to conclude that any metallic area from original alloy samples is exposed.

The release profiles were very similar to pure ceramics and polymers matrixes. Figures 5, 6 and 7 shows the cumulative amount of gentamicin released versus time and its standard deviation multiplied by 10 ( $\pm 10$  SD). Each

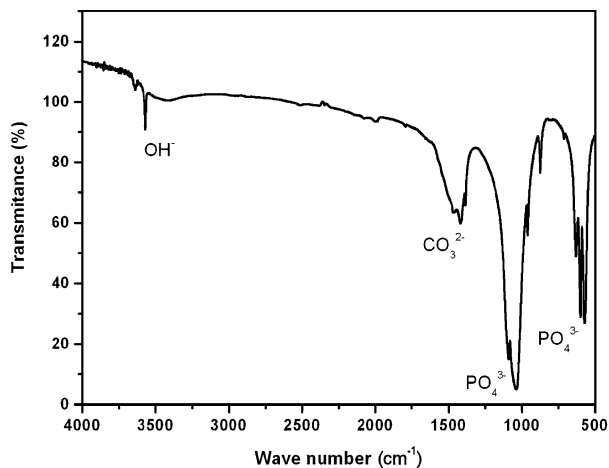


Fig. 1 FTIR spectrum for the coatings on Ti–Al–V

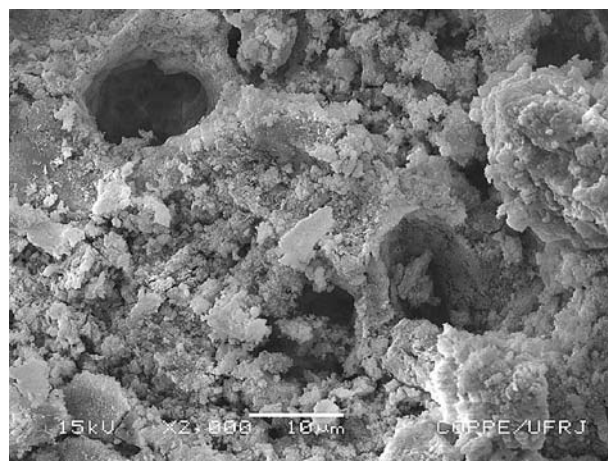


Fig. 3 SEM micrography of HA coating

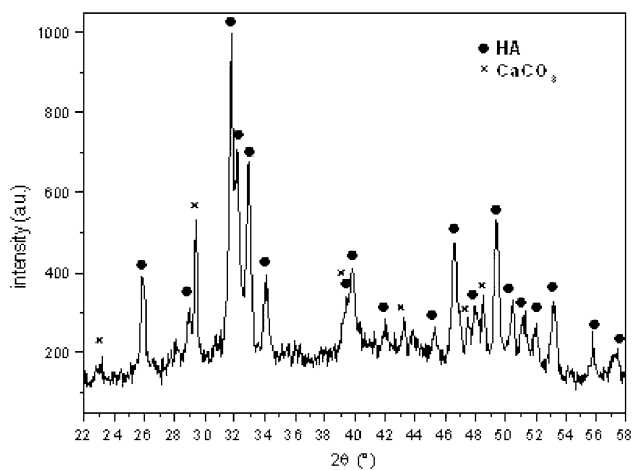


Fig. 2 XRD pattern of the coating obtained by sol-gel

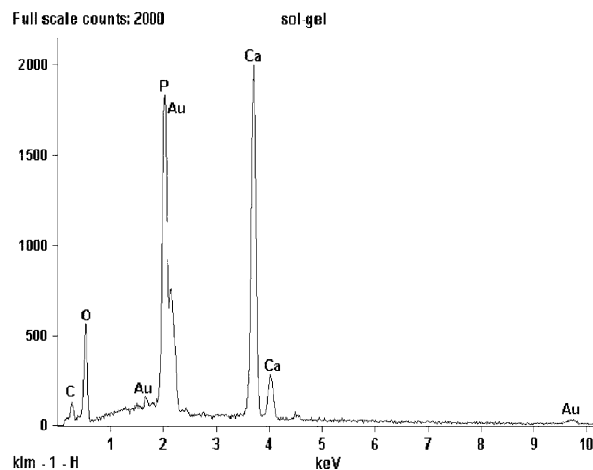
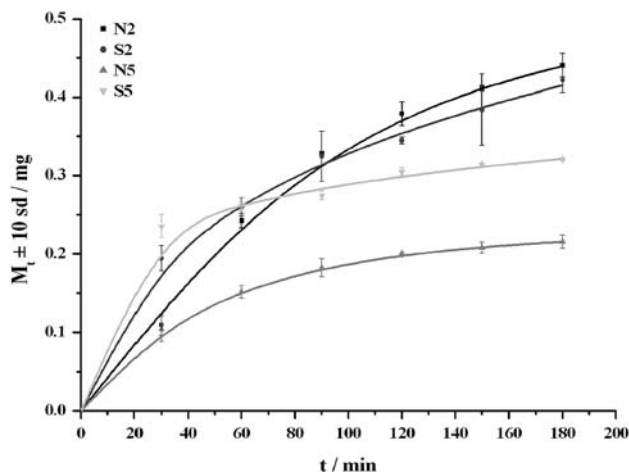
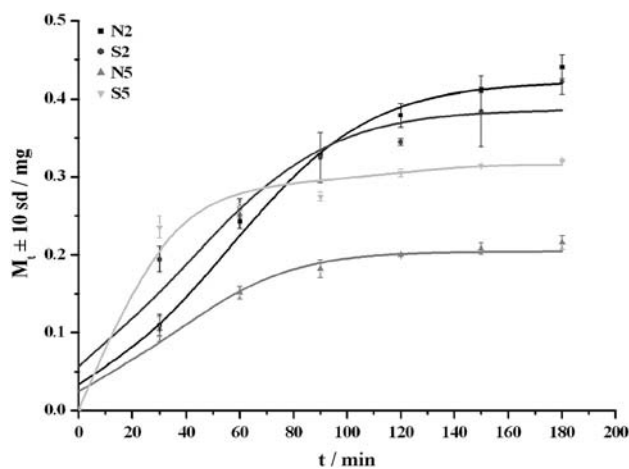


Fig. 4 EDS analysis of sol-gel HA coating onto Ti–Al–V alloy



**Fig. 5** Fitting to Weibull distribution



**Fig. 6** Fitting to logistic function

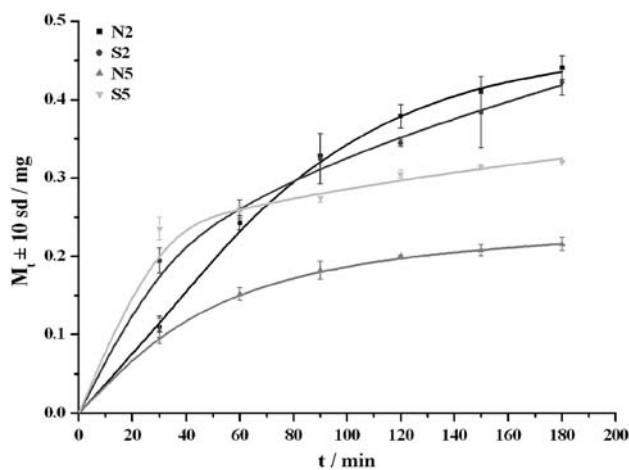


**Fig. 7** Fitting to Torrado and Frutos equation

point in the plot represents the mean of five independent experiments and the scatters shows the experimental data and lines the fitting models. There is a very small

dispersion of the data despite with the literature [14, 15]. From these results we can conclude that the method of producing the specimens is not responsible for the possible erratic release although in other kind of non-metallic matrix. In can be observed that the remanent solution keep clear, while the samples made with stirring the same solutions were turbid [15]. It may be due to the fact that only gentamicin molecules located in the superficial layers of the device system are accessible through voids and cracks to the dissolution medium, since as will be discussed later, gentamicin cannot cross the very interconnected porous network of the HA coating because the gentamicin molecule, very large in size, dissolved in the aqueous dissolution medium is not able to diffuse through the HA coating.

For analyzing release curves by mathematical models, several criteria were considered such as a graphical representation. In Figs. 5, 6 and 7, a good agreement can be observed between experimental and fitted points. The degree of fit was quantified by determination coefficient ( $R^2$ ), the sum of squares residuals (SSR) and the AIC (Table 1). Another point of view was the estimated parameters and their standard error ( $\pm$ SE) shown in Table 2 and finally the physical relevance of the estimated parameters. The order established for the incident factors is according to the importance of the answer to obtain. For example, is very relevant that the experimental data and the model have a good agreement, as shown Figs. 5, 6 and 7.

**Table 1** Statistical criteria ( $N = 7$ )

Model	Code	$R^2$	SSR	$p$	AIC
Eq. 1	N2	99.660	5.5723	3	18.0
	S2	99.777	2.7465	3	13.1
	N5	99.979	0.0764	3	-12.0
	S5	99.801	$1.5 \times 10^{-4}$	3	-55.6
Eq. 2	N2	98.563	23.525	3	28.1
	S2	93.560	79.362	3	36.6
	N5	96.210	13.545	3	24.2
	S5	96.380	27.275	3	29.1
Eq. 3	N2	99.935	1.0606	4	8.41
	S2	99.808	2.3568	4	14.0
	N5	99.969	0.1082	4	-7.57
	S5	99.843	1.1830	4	9.18

**Table 2** Parameters of the release profiles from Weibull distribution

Model	Code	$M_\infty \pm SE$	$\alpha \pm SE$	$\beta \pm SE$
Weibull	N2	$49 \pm 5$	$0.006 \pm 0.003$	$1.1 \pm 0.1$
	S2	$80 \pm 40$	$0.04 \pm 0.01$	$0.6 \pm 0.1$
	N5	$22.7 \pm 0.3$	$0.030 \pm 0.003$	$0.88 \pm 0.03$
	S5	$1 \pm 7$	$0.1 \pm 0.7$	$0.2 \pm 0.2$



The statistical results confirm the possible selection made from the graphics and in fact, allows the more adequate physical interpretation of the phenomena.

One of the objectives of this contribution was to elucidate the drug transport mechanism involved in the release of a drug from HA coatings. A non-linear least-squares regression was performed and the model parameters were calculated. Also, the AIC and the SSR (Table 1) were determined for each model as they are indicators of the model suitability for a given data set, as discussed earlier [11].

Notice that Torrado and Frutos equation was a good fitting, but the four incident factors lead us to select the Weibull distribution to because is a function widely known and used in drug release systems despite the matrix [10]. Besides, the Torrado and Frutos equation is the Kuhn and Wilson rewritten in order to explain the phenomenon from hydrophobic polymeric matrix, while the Weibull distribution allows more adequate physical interpretation of the parameters due to  $\alpha$  and  $\beta$ , depends on the range and time units for  $\alpha$  and the curve shape for  $\beta$ . From this point of view, the best fitting was obtained with the Weibull function. The plot of the cumulative amount of drug dissolved against time can be described by the Eq. 1 and the physical significance of the parameters was enunciated above. The values are shown in Table 2.

In our case, the  $\beta$  values were very close to 1 according to the curve shape (Fig. 5). The  $\alpha$  values were very lower than reported in literature, may be due to change in the matrix. There exists a few reports about the drug release from HA coatings over metallic substrates, and is very difficult to compare without information. The result for S5 confirms the selection of the appropriate methodology to dope the recovered metallic substrates. In the literature, values for  $\alpha$  vary between 0.03 and 2.1 and for  $\beta$  among 0.4 and 1.75 [10]. Of course, these parameter values also depend on the range and time units (hours, minutes) used. In addition, may be the higher difficulty of the non-linear methods is the selection of the parameters values to begin the iterations. From that, the importance to select models which parameters with physical sense. The ending evaluation of the release process correspond to a mixture of an initial burst effect, follows of the combined effect of the drug dissolution with a specific kinetic very dependent of the shape of the release profile, with an 20–40% of the drug delivered in 3 h, but a significant slope indicated that a process continue.

#### 4 Conclusions

The work thus far undertaken has illustrated that it is possible to produce HA via sol–gel method. Porous HA films were deposited on Ti–Al–V substrates using sol–gel

route, and novel heat treatment at 450°C. Both XRD and FTIR show that the films exhibit crystalline apatitic structure. The sol–gel HA coatings are firmly attached to the sand blasted Ti–Al–V substrate, through both mechanical interlocking and possibly certain degree of chemical bonding. The presence of HA coatings over the passive layer makes the metal surface more bioactive. The samples release 30–40% in 3 h through a complex mechanism that fulfilled the Weibull distribution according the AIC. Considering the simplicity of the sol–gel dip-coating method and the good interfacial strength of the resulting HA films, sol–gel processing offers a promising approach for modifying the surface of load-bearing implants intended for bone-interfacing applications and they are potential drug release matrixes in order to avoid the possible infection in the implant site.

**Acknowledgments** The authors thank the financial support of the cooperative project between CNPq/Brasil and MES/Cuba “Desarrollo de un recubrimiento a base de HAP y polímeros cargados con medicamentos sobre sustratos metálicos”. They also thank the Inorganic Chemistry Department/IQ/UFRJ for UV spectroscopy and Centro Brasileiro de Pesquisa Física, CBPF, for infrared spectroscopy and XRD services.

#### References

1. W. Diangang, C. Chuangzhong, X. Liu, L. Tingquan, *Colloids Surf. B Biointerfaces* **57**, 237 (2007). doi:10.1016/j.colsurfb.2007.02.003
2. D.M. Liu, T. Troczynski, W.J. Tseng, *Biomaterials* **23**, 1227 (2002). doi:10.1016/S0142-9612(01)00242-3
3. D.M. Liu, Q. Yang, T. Troczynski, W.J. Tseng, *Biomaterials* **23**, 1679 (2002). doi:10.1016/S0142-9612(01)00295-2
4. J. Hill, L. Klenerman, S. Trustey, R. Blowers, *J. Bone Joint Surg.* **59B**, 197 (1977)
5. S. Torrado, P. Frutos, *Int. J. Pharm.* **217**, 57 (2001). doi:10.1016/S0378-5173(01)00587-7
6. M.G. Diniz, M.S. Sader, G.A. Soares, *Brazilian Dental Mag. Ver. RBO* **58**, 135 (2001)
7. R. Denoyel, M.T.J. Keene, P.L. Llewellyn, J. Rouquerol, *J. Therm. Anal. Calorim.* **56**, 261 (1999). doi:10.1023/A:1010165626343
8. F. Langenbucher, *J. Pharm. Pharmacol.* **24**, 979 (1972)
9. J.T. Carstensen, *Pharmaceutics of Solids and Solid Dosage Forms* (New York, Wiley, 1977), pp. 63–76
10. E. Adams, D. Coomans, J. Smeyers-Verbeke, D.L. Massart, *Int. J. Pharm.* **240**, 37 (2002). doi:10.1016/S0378-5173(02)00127-8
11. L. Serra, J. Domenech, N.A. Peppas, *Biomaterials* **27**, 5440 (2006). doi:10.1016/j.biomaterials.2006.06.011
12. E. Peon, G. Fuentes, J.A. Delgado, L. Morejon, A. Almirall, R. García, *Lat. Am. Appl. Res.* **34**(4), 225 (2004)
13. B.O. Fowler, *J. Inorg. Chem.* **13**, 194 (1974). doi:10.1021/ic50131a039
14. M. Stitger, K. de Groot, P.L. Ayrolle, *Biomaterials* **23**, 4143 (2002). doi:10.1016/S0142-9612(02)00157-6
15. F. X. Gil, in *Liberación de fármacos en matrices biocerámicas: Avances y perspectivas Monografía XIX*, ed. by M. Vallet Regí, A.L. Doadrio (Real Academia de Farmacia, Realigraf SA Madrid, 2001), pp. 173–202